THRUST REVERSER AERODYNAMIC DESIGN:

CFD ANALYSIS AND COMPARISON WITH EXPERIMENTS

D. Kliche[1], R. Spieweg[2], R. Schweikhard[2], Ch. Mundt[1]
[1] Universität der Bundeswehr München / Institute of Thermodynamics
85577 Neubiberg / Germany
[2] Rolls-Royce Deutschland Ltd. & Co. KG
15827 Dahlewitz / Germany

ABSTRACT

In the design process of thrust reverser systems for civil turbofan powerplants using pivoting doors like the Rolls-Royce BR710 and BR715, a compromise between powerplant performance in forward and reverse thrust mode has to be found. So far, design, development and the quantification of powerplant performance (measured in terms of discharge and thrust coefficient C_D and C_V) was mainly derived from model tests. This paper presents a numerical study using 3D Reynolds averaged Navier-Stokes (RANS) calculations to support the development of a new application whose thrust reverser design depends on the use of CFD (Computational Fluid Dynamics) to a higher extent than in earlier cases. CFD results of forward and reverse thrust mode configurations were analysed and compared with experimental data. The main goal was the performance optimisation of pit cavity, fan ramp and kicker plate shapes. CFD results correlate well with experiments and reproduce features like suppression effects due to increasing free stream velocity as well as the characteristic difference between model and full scale performance parameters.

NOMENCLATURE

Symbol	Unit	Description
A	[m^2]	Area
c	[m/s]	Velocity
C_D		Discharge coefficient
C_V		Thrust coefficient
D	[N]	Drag
F	[N]	Force
F_G	[N]	Gross thrust
F_N	[N]	Net thrust
$\dot{m}$	[kg/s]	Mass flow rate
$\vec{n}$		Normal vector
p	[Pa]	Pressure
Q	$\left[\sqrt{K}s/m\right]$	Reduced mass flow
R	[J/(kg K)]	Gas constant
T	[K]	Temperature
γ		Ratio of specific heats
ρ	[kg/m^3]	Density
σ	[Pa]	Surface force density

Subscript	Description
0	Intake stream tube inlet
01	Intake stream tube outer surface
9	Exit of nozzle
∞	Ambient condition
eff	Effective
ref	Reference
t	Total state
x	In x-Direction
*	Critical state

1. INTRODUCTION

Rolls-Royce Deutschland has developed new, efficient and environmentally friendly propulsion systems for long distance corporate and for regional aircraft. Both, the BR710 and BR715 turbofan engines are equipped with forced mixers and a mixed flow exhaust system supporting an efficient thrust reverser using pivoting doors as shown in FIG 1. However, continuous effort is necessary to further develop the powerplants in order to meet customer requests.

Thrust reverser systems are generally an integral part of civil turbofan engines. Primarily they support the wheel brakes in slowing down an aircraft during a regular landing or in an emergency situation. In doing so the engine flow is deflected by so-called cascades or blocker doors in a way that a force opposite to the intrinsic thrust is generated.

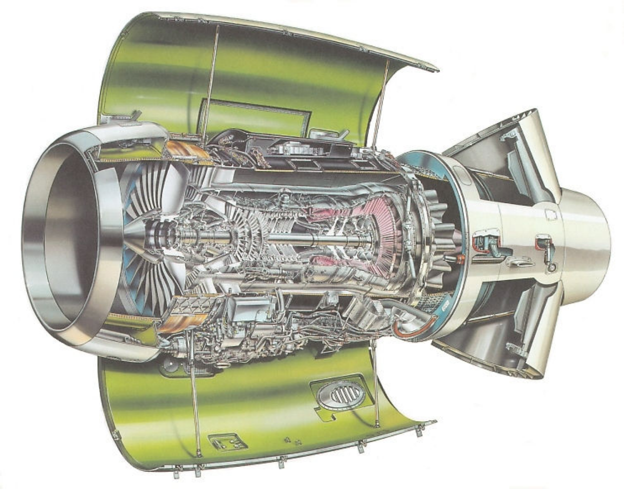

FIG 1. Rolls-Royce BR710 engine with deployed pivot door thrust reverser.

In today's mixed turbofan engines the so-called pivoting doors are used often to deflect both the engine core and fan (bypass) gas flow as efficiently as possible[1]. Moreover, the closed pivoting doors build the nozzle contour in the forward thrust mode, where small losses and such a high efficiency are recommended. The main parts of a thrust reverser system with open pivoting door are presented schematically in FIG 2.

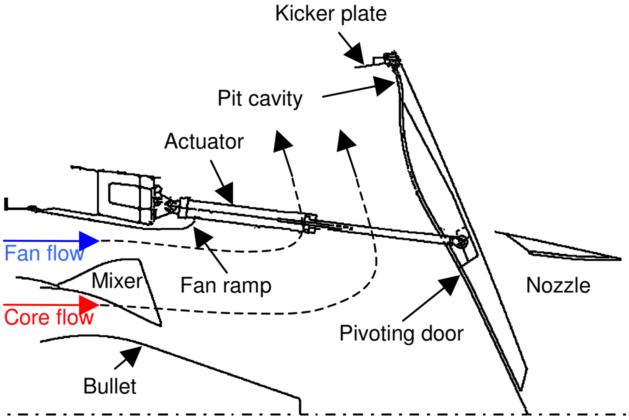

FIG 2. Schematic diagram of a thrust reverser system with pivoting doors.

The flow in a thrust reverser is of high complexity and depends on numerous geometric details. Thus the design and development of a thrust reverser and the quantification of its performance (in forward as well as in reverse mode) was so far mainly depending on model and engine testing. Today's possibilities in using CFD offer the potential for a detailed design and optimisation of the thrust reverser in an early stage of the development process, before the design space for geometric changes becomes more and more restricted[2]. Hence, testing might be used for validation rather than for development, which reduces risks, time and costs.

This paper presents a numerical study using 3D RANS calculations to support the development of a new powerplant whose thrust reverser design depends on the use of CFD to a higher extent than in earlier cases. To this end the test results of the BR710 engine were used for validation purpose, before using this approach for designing the new powerplant. Full scale and 1/5th scale models of the flow around and through powerplants half models in forward and reverse thrust mode have been simulated at different free stream velocities to compare with model test results. The main focus of the investigations reported here lies on the influence of fan ramp and pit cavity shape on the performance parameters in forward and reverse thrust mode. Thus, variations of the thrust and discharge coefficients C_V and C_D for different geometries are shown.

2. COMPUTATIONAL MODEL

Two general configurations, one for the forward thrust mode and one for the reverse thrust mode have been analysed using the commercial RANS solver *FLUENT 6.2*[3]. As mentioned before, 3D full scale and 1/5th scale powerplant half models have been simulated (see FIG 3 to FIG 5). In addition, simplified axisymmetric calculations for the forward thrust mode have been performed. Turbulence was taken into account applying the realizable k-ε model[4] and additionally for the axisymmetric simulations the shear-stress transport (SST) k-ω model[5].

The hybrid grids for the 3D models have been generated with *CENTAUR*^{TM} software[6]. For the forward thrust mode the grid contains approximately 1.2 million nodes with 4 million cells. The geometric configuration with nacelle walls, closed pivoting door, forced mixer, bullet and the numerical inlets for core and fan mass flow is illustrated in FIG 3.

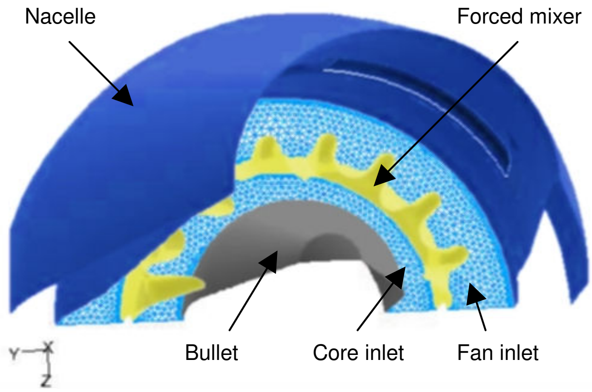

FIG 3. Upstream view from aft of the nozzle showing the configuration of the forward thrust CFD model.

For comparability to the cold flow experiment the entry temperatures for the core and fan flow were set accordingly and the air was modelled as ideal gas with constant gas properties and the Sutherland equation to calculate viscosity. For the sake of completeness FIG 4 shows a contour plot of the Mach number in the centre plane of the powerplant.

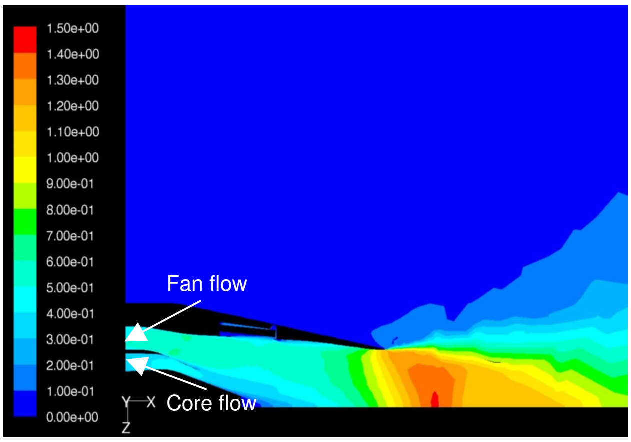

FIG 4. Contours of Mach number in the centre plane in forward thrust mode.

The hybrid mesh set up for the reverse thrust mode simulations consisted of approximately 2.2 million nodes and 6.1 million cells. The calculation took about two days on a *SGI Altix 3700* in parallel mode on 8 processors[1].

Both geometries were built as half-models because of the asymmetric nozzle, which generates a slightly deflected thrust vector. Compared to the forward mode model the reverse one also included the nacelle inlet. FIG 5 shows some streamlines and illustrates the computational domain for the reverse thrust mode for convenience.

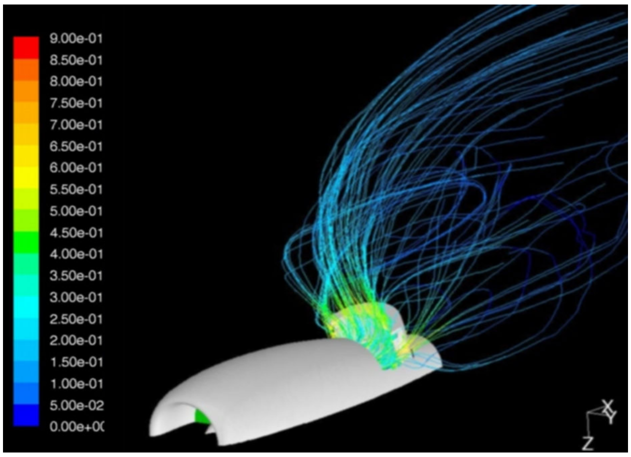

FIG 5. Streamlines coloured by Mach number of the gas flow in reverse thrust mode.

The powerplant inlet was modelled as a numeric (pressure) outlet and the numeric inlets for the core and fan flow were modelled as numeric (pressure) outlets and placed upstream of the mixer equal to those in forward thrust mode (compare to FIG 3). Due to the hot core mass flow the gas was modelled with piecewise polynomial equations for the gas properties. FIG 6 shows a contour plot of the Mach number in the centre plane of the powerplant and highlights the numeric inlet and outlets of the fan and core flows.

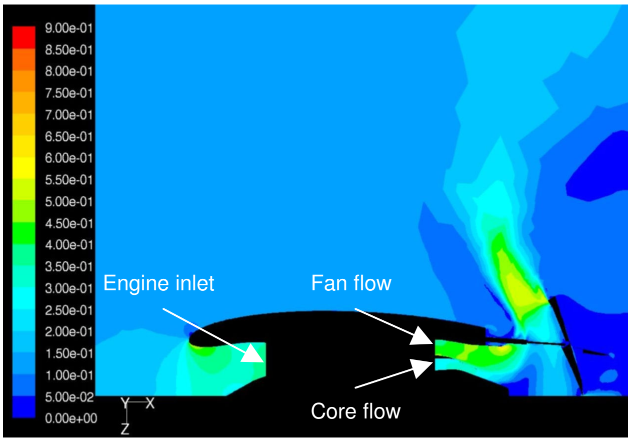

FIG 6. Contours of Mach number in the centre plane in reverse thrust mode.

3. PERFORMANCE ANALYSIS

Based on the computational models described in chapter 2 an adequate analysis for the performance parameters in forward and reverse thrust mode had to be derived. Therefore, a control volume was defined to determine the balance force F_x as a function of either gross thrust F_{Gx} or net thrust F_{Nx}. The control volume is made up from the intake capture stream tube (A_0, A_{01}), the external nacelle walls $A_{Nacelle}$, the distributed exit surface A_9 and the external thrust reverser door base A_{Base} presented in FIG 7.

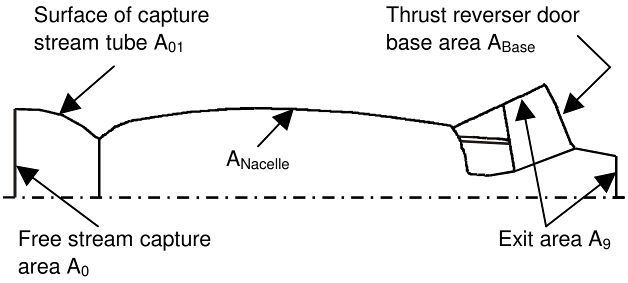

FIG 7. Control volume for determination of gross and net thrust in forward as well as in reverse mode.

[1] Itanium2 "Madison", 1.5 GHz.

The momentum balance in x-direction around the control volume yields:

$$(1)\quad \begin{aligned} F_x = &\int_{A_9} (p-p_\infty)\, n_x dA + \int_{A_9} \rho c_x (\vec{c}\cdot\vec{n})\, dA - \\ &\int_{A_0} \rho c_x^2\, dA + \int_{A_{01}} (p-p_\infty)\, n_x\, dA - \int_{A_{Nacelle+Base}} \sigma_x\, dA \end{aligned} .$$

With the definition of the gross thrust F_{Gx} (2) and net thrust F_{Nx} (3) from reference [1]

$$(2)\quad F_{Gx} = \int_{A_9} (p-p_\infty)\, n_x dA + \int_{A_9} \rho c_x (\vec{c}\cdot\vec{n})\, dA$$

$$(3)\quad F_{Nx} = F_{Gx} - \int_{A_0} \rho c_x (\vec{c}\cdot\vec{n})\, dA = F_{Gx} - \dot{m} c_\infty ,$$

equation (1) gives the following expression for the gross thrust F_{Gx}, where the balance force F_x can be calculated regarding a control volume bordered by the inner and outer walls, the numeric inlets and outlets and the intake stream tube. The ram drag ($\dot{m} c_\infty$) and the surface forces $D_{Nacelle+Base}$ can be determined by evaluating the flows and body forces obtained from the CFD results.

$$(4)\quad F_{Gx} = F_x + \dot{m} c_\infty + D_{Pre-entry} + D_{Nacelle+Base} .$$

In addition to the gross thrust the discharge and thrust coefficients C_D and C_V respectively are generally used in powerplant performance analysis. From reference [7] the discharge coefficient C_D is defined as the ratio of the measured mass flow to the ideal mass flow

$$(5)\quad C_D = \frac{\dot{m}}{\dot{m}_{ideal}} = \frac{1}{A} \frac{\dot{m}\sqrt{T_t}/p_t}{Q_{ideal}} ,$$

where the reduced mass flow or Q-function Q is given by:

$$(6)\quad Q = \frac{\dot{m}\sqrt{T_t}/p_t}{A} .$$

This definition for C_D is applicable for a single stream exiting the nozzle. In case of mixed streams leaving the nozzle it is common practice to define the discharge coefficient as the ratio of effective area to geometric area. Effective areas ($A_{eff}=C_D$*A) are computed according to the above definition of the discharge coefficient based on measured/computed mass flows. Thus, the discharge coefficient for mixed streams can be calculated with the following expression[7]:

$$(7)\quad C_D = \frac{\sum A_{eff}}{A} = \frac{1}{A}\left[\left(\frac{\dot{m}\sqrt{T_t}/p_t}{Q_{ideal}}\right)_{Fan} + \left(\frac{\dot{m}\sqrt{T_t}/p_t}{Q_{ideal}}\right)_{Core}\right].$$

The thrust coefficient C_V as used here is defined, as the ratio of measured gross thrust (compare with equation (4)) to measured mass flow times the ideal velocity c_{ideal}. Latter is calculated by the equation of de Saint-Venant and Wantzel[1] for the exhaust velocity from a vessel. Using the reduced mass flow (6), the thrust coefficient for a single stream is given by following equation[7]:

$$(8)\quad C_V = \frac{F_{GX}}{\dot{m} c_{ideal}}$$

$$C_V = \frac{F_{GX}}{\dot{m}\sqrt{T_t}\, QR(p_t/p)^{1/\gamma}} \text{ with } \begin{cases} p_t/p \le p_t/p^* \rightarrow p = p_\infty \\ p_t/p > p_t/p^* \rightarrow p = p^* \end{cases} .$$

Corresponding to the discharge coefficient the thrust coefficient for mixed flows exiting the nozzle is calculated using equation (9)[7]:

$$(9)\quad C_V = \frac{F_{GX}}{\left(\dot{m}\sqrt{T_t}\, QR(p_t/p)^{1/\gamma}\right)_{Fan} + \left(\dot{m}\sqrt{T_t}\, QR(p_t/p)^{1/\gamma}\right)_{Core}} .$$

4. FORWARD THRUST MODE CFD

As mentioned before, fan ramp and pit cavity designs (see FIG 2) affect the performance in reverse thrust as well as in forward thrust mode. Therefore, an axisymmetric parametric analysis has been set up to study the interaction of the shape of the pivoting doors and the recirculation zone with the fan ramp. Three configurations with pit cavity and one without for reference have been analysed, each with approximately 200,000 nodes on a structured grid. The maximum depth of the pit cavities has been the same for all three cases. Configurations a) with a short pit cavity and a sharp fan ramp, b) with a long shallow pit cavity and a sharp fan ramp and c) with a long shallow pit cavity and a smooth fan ramp are shown in FIG 8. Wall streamlines define the size of the recirculation zone, which is of high impact on the performance of the exhaust system.

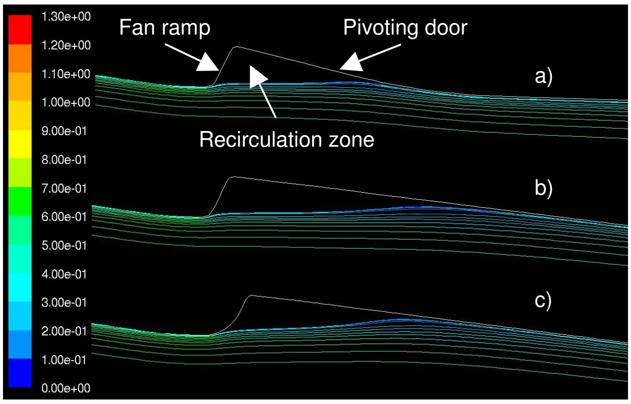

FIG 8. Wall-streamlines coloured by Mach number for a) the short pit with sharp fan ramp; b) the long shallow pit with sharp fan ramp; c) the long shallow pit with smooth fan ramp.

Comparing the total pressure losses it was found that a reduction of the recirculation zone is beneficial for forward mode performance. The highest pressure recovery and the smallest recirculation zone, respectively was achieved within configuration c) the long shallow pit with the smooth fan ramp for the realizable k-ε turbulence model. For the shear-stress transport (SST) k-ω turbulence model, configuration a) has the best performance regarding total pressure losses.

From these results a general trend for the total pressures could be observed between the two turbulence models. Thus, a constant deviation was found. TAB 1 summarises the computed configurations and compares the mass averaged total pressures computed with *FLUENT* at the nozzle exit. Additionally, the total pressures are plotted in FIG 9 to illustrate the constant deviation between the two turbulence models for the three configurations a) – c) and the clean configuration d).

Case	Turbulence model	Normalized mass averaged total exit pressure
d) No pit	Realizable k-ε	0.9880
d) No pit	SST k-ω	0.9866
a) Sharp ramp short pit	Realizable k-ε	0.9875
a) Sharp ramp short pit	SST k-ω	0.9851
b) Sharp ramp long pit	Realizable k-ε	0.9858
b) Sharp ramp long pit	SST k-ω	0.9836
c) Smooth ramp long pit	Realizable k-ε	0.9878
c) Smooth ramp long pit	SST k-ω	0.9844

TAB 1. Results of the axisymmetric configurations for the forward thrust mode.

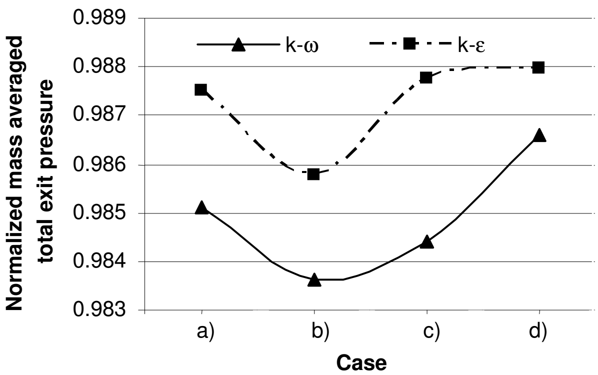

FIG 9. Total pressures calculated with the realizable k-ε and the SST k-ω turbulence model for a) short pit with sharp fan ramp; b) long shallow pit with sharp fan ramp; c) long shallow pit with smooth fan ramp; d) reference case without pit cavity.

It can be stated from these results, that a deep pit not necessarily results in high forward mode losses but could be optimised together with the fan ramp shape. The increased depth could be used to lengthen the kicker plates to gain reverse efficiency. Furthermore, extended kicker plate length increases the potential for kicker plate variation with respect to optimisation of area match and efflux control. A possible variation of the thrust reverser pit cavity shape is sketched in FIG 10.

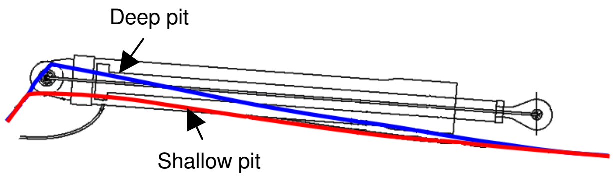

FIG 10. Possible variation of thrust reverser doors pit cavity shape.

Moreover, another characteristic connected to the fan ramp shape can be observed regarding oil flow visualizations and 3D CFD computations. Functionally the flow is only turned outwards in the pivoting door's centre part. But by extending the smooth portion of the fan ramp circumferentially the flow in this region will be deflected to a greater extent. This will lead to an increase in reverse C_D by the expense of reverse C_V. Recalling the axisymmetric results presented above, a smooth extended fan ramp might also result in an improved forward mode performance. However, moving from the 2D view to a 3D design as illustrated in FIG 12 other considerations come into play. Here the smoothed delta region induces cross flow, which leads to longitudinal vortices at the cavity sides causing additional losses in forward mode. The fan ramp and the possible circumferential extension in its delta region are shown in an oil flow picture in FIG 11. The oil flow visualizations conducted with a 1/5th scale model show a good correlation between experiments and 3D CFD. Overall, the sharp fan ramp shows better forward mode performance.

FIG 11. Oil flow experiment showing fan ramp effectiveness.

A possible variation of the fan ramp smoothness is shown in FIG 12 illustrating the complexity of a 3D fan ramp design. Here the sharp version leads to improvements for the forward and reverse mode.

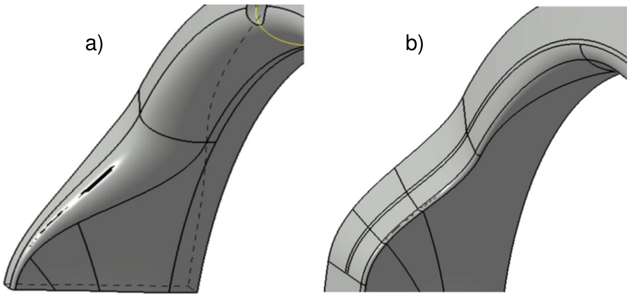

FIG 12. a) Smooth circumferential extension of fan ramp; b) Sharp circumferential extension of fan ramp.

FIG 13 shows the forward mode performance difference for model test and CFD in terms of ΔC_D (scaled with the BR710 model test ΔC_D) and ΔC_V (scaled with the BR710 model test ΔC_V) between clean jet pipe and pit cavities included. The prediction accuracy for ΔC_V - the most important parameter - is excellent keeping in mind that these are very small numbers. As can be seen, the absolute delta is slightly improved on the new design. It also appears that the tested ΔC_D for BR710 are smaller than those evaluated from the CFD, which might be explained with the small number of tested data points and the relatively high data scatter.

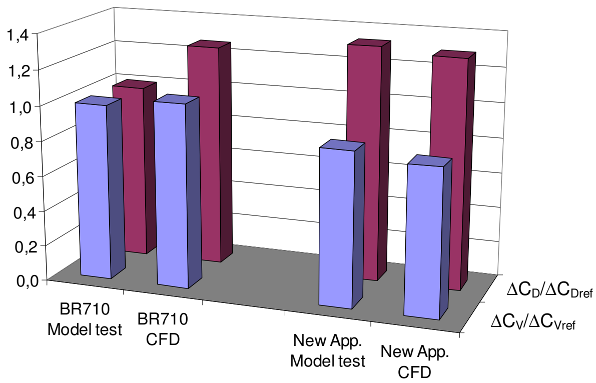

FIG 13. ΔC_D and ΔC_V between clean jet pipe and pit cavities included designs for the BR710 and the New Application scaled with BR710 forward model test data.

5. REVERSE THRUST MODE CFD

In reverse thrust mode the BR710 powerplant geometry has been used to study the difference between full scale and 1/5th model scale and the effect of free stream velocity on the performance parameters introduced in chapter 3.

Calculations with 10.3m/s (20knots) and 51.4m/s (100knots) free stream velocity for each the full scale and the 1/5th model scale have been performed. With the 10.3m/s case the free stream velocity has been set as small as possible to guarantee a stable CFD solution and to match with the experiments, which were conducted with a 1/5th scaled model in a static test facility i.e. without flight velocity representation. From the CFD results presented in FIG 14 it can be seen that the scaling significantly affects the discharge coefficients at 10.3m/s free stream velocity by about 1.7% relative. For the 51.4m/s case only a small difference was found between the two cases. The differences between thrust coefficients (compare to FIG 14) are approximately 10% of the measured BR710 reverse thrust. This effect was earlier observed between full scale powerplants and downscaled models, thus corresponding well with experimental data.

FIG 14 also indicates a reduction of C_D with increasing free stream velocity, which is due to a so-called suppression effect. Hence, the higher the free stream velocity the higher the suppression on the powerplant efflux leading to a decreased effective area.

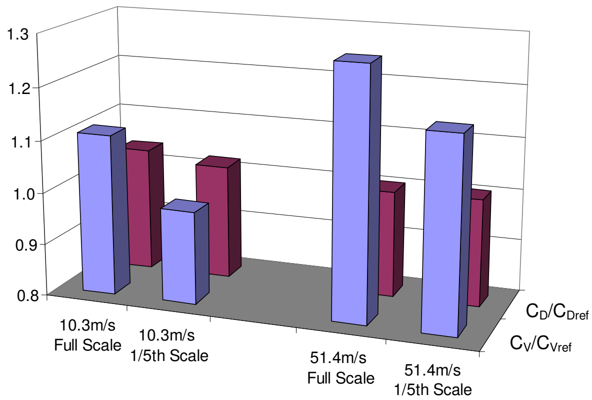

FIG 14. C_D and C_V for different free stream velocities c_∞ and different scales from BR710 reverse thrust mode CFD scaled with BR710 reverse model test data.

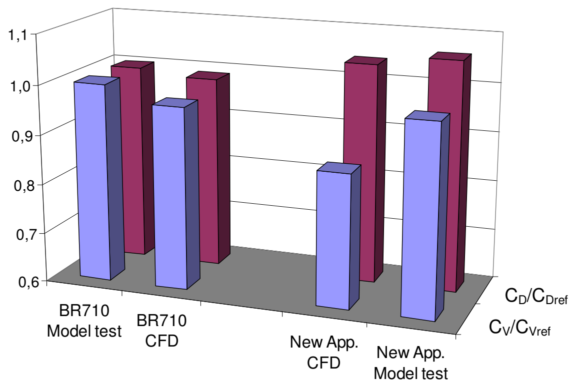

FIG 15. Comparison of experimental to numerical coefficients scaled with BR710 reverse model test data showing design differences and prediction capability.

The comparison of CFD to model test data shows a consistent and small ΔC_D, as can be seen in FIG 15. However, the comparison of C_V exhibits differences on a larger scale. For that purpose, a CFD validation campaign is ongoing. Nevertheless, the prediction of mass flows - important for the assessment of working lines - is sufficiently accurate to determine design differences between the BR710 thrust reverser and new designs. Test results of the new design show that significantly larger discharge is achieved at only a slightly lower C_V.

In general thrust reversers are operated above a certain aircraft speed to prevent reingestion of the efflux. Below that speed the reverse thrust is continuously reduced to reverse idle[1]. The streamlines of the effluxes for c_∞ = 10.3m/s and c_∞ = 51.4m/s are visualized in the following figures FIG 16 and FIG 17 for convenience.

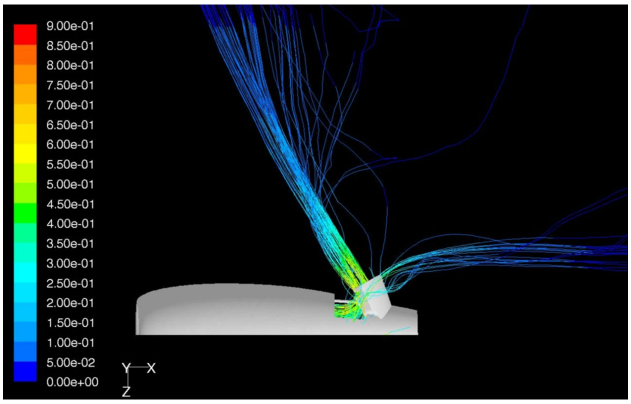

FIG 16. Streamlines coloured by Mach number of efflux in reverse thrust mode at c_∞ = 10.3m/s (20knots).

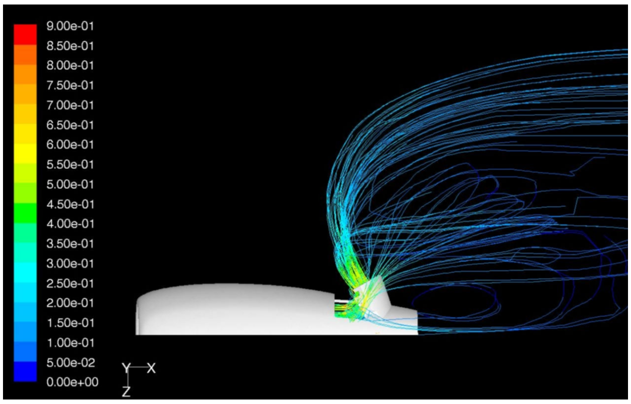

FIG 17. Streamlines coloured by Mach number of efflux in reverse thrust mode at c_∞ = 51.4m/s (100knots).

6. CONCLUSIONS

A numerical study using 3D RANS calculations has been carried out at the Universität der Bundeswehr München in cooperation with Rolls-Royce Deutschland Ltd. & Co. KG to support the development of a new powerplant whose thrust reverser design depends on the use of CFD to a higher extent than in earlier cases. Today's possibilities in using CFD offer the potential for a detailed design and optimisation of the thrust reverser in an early stage of the development process, before the design space for geometric changes becomes more and more restricted. Hence testing might be used for validation rather than for development, which reduces risks, time and costs.

Full scale and 1/5th scale models of the flow around and through powerplants half models in forward and reverse thrust mode have been simulated at different free stream velocities to compare with model test results. Thrust and discharge coefficients C_V and C_D show significant variation with different geometries. Thus, the size of the recirculation zone has the greatest influences on the performance in forward thrust mode. Since the recirculation zone and the pit cavity and fan ramp respectively influence the length of the thrust reverser's kicker plate and in turn the kicker plate's length affects the reverse thrust mode performance, an optimum for the required standards for forward and reverse thrust mode has to be found. Thus the pit cavity and fan ramp should not be designed independently.

Recapitulating, the following statements can be concluded:

- Using CFD to design fan ramp, kicker plates as well as the pit cavity, the best overall compromise between aerodynamic and structural considerations is found.
- CFD correlates well with experiments and is used to support the development of new powerplants.
- Suppression effects in reverse thrust mode caused by increasing free stream velocity and differences in model scale to full scale are reproduced using CFD.
- Although longer kicker plates would be beneficial for reverse Cv and efflux control, the benefits of a shallow pit in forward mode dominate the choice for shorter kicker plates.
- The fan ramp has to be designed accordingly to the pit cavity.

7. REFERENCES

[1] W. J. G. Bräunling: Flugzeugtriebwerke; Springer-Verlag, 2004.

[2] D. J. Strash, J. M. Summa, J. H. Frank, R. Standish: Aerodynamic Analysis of an Installed Thrust Reverser; Journal of Propulsion and Power, 0748-4658 vol.16 no.1 (10-15), 2000.

[3] FLUENT Incorporated: FLUENT 6.2 Documentation; 2005.

[4] T.-H. Shih, W. W. Liou, A. Shabbir, Z. Yang, J. Zhu: A New - Eddy-Viscosity Model for High Reynolds Number Turbulent Flows - Model Development and Validation; Computers Fluids, 24(3):227-238, 1995.

[5] F. R. Menter, M. Kuntz, R. Langtry: Ten Years of Experience with the SST Turbulence Model; In K. Hanjalic, Y. Nagano, M. Tummers, editors, Turbulence, Heat and Mass Transfer 4; pages 625-632. Begell House Inc., 2003.

[6] CentaurSoft: CENTAUR™ online manual; 2007. http://www.centaursoft.com/

[7] J. D. Mattingly, W. H. Heiser, D. H. Daley: Aircraft Engine Design, AIAA Education Series, 1987.